



# Equivalent ambipolar carrier injection of electrons and holes with Au electrodes in air-stable field effect transistors

Cite as: Appl. Phys. Lett. **107**, 043304 (2015); <https://doi.org/10.1063/1.4927651>

Submitted: 01 May 2015 . Accepted: 19 July 2015 . Published Online: 29 July 2015

Thangavel Kanagasekaran, Hidekazu Shimotani, Susumu Ikeda , Hui Shang, Ryotaro Kumashiro, and Katsumi Tanigaki 



View Online



Export Citation



CrossMark

## ARTICLES YOU MAY BE INTERESTED IN

[Green light emission from the edges of organic single-crystal transistors](#)

Applied Physics Letters **97**, 173301 (2010); <https://doi.org/10.1063/1.3504690>

[Very high-mobility organic single-crystal transistors with in-crystal conduction channels](#)

Applied Physics Letters **90**, 102120 (2007); <https://doi.org/10.1063/1.2711393>

[Organic electroluminescent diodes](#)

Applied Physics Letters **51**, 913 (1987); <https://doi.org/10.1063/1.98799>



Lock-in Amplifiers

Zurich Instruments

Watch the Video 

## Equivalent ambipolar carrier injection of electrons and holes with Au electrodes in air-stable field effect transistors

Thangavel Kanagasekaran,<sup>1,a)</sup> Hidekazu Shimotani,<sup>2,a)</sup> Susumu Ikeda,<sup>1</sup> Hui Shang,<sup>2</sup> Ryotaro Kumashiro,<sup>1</sup> and Katsumi Tanigaki<sup>1,2,a)</sup>

<sup>1</sup>WPI-Advanced Institute for Materials Research (WPI-AIMR), Tohoku University, 2-1-1 Katahira, Aoba, Sendai 980-8577, Japan

<sup>2</sup>Department of Physics, Graduate School of Science, Tohoku University, 6-3 Aoba, Aramaki, Aoba, Sendai 980-8578, Japan

(Received 1 May 2015; accepted 19 July 2015; published online 29 July 2015)

Carrier injection from Au electrodes to organic thin-film active layers can be greatly improved for both electrons and holes by nano-structural surface control of organic semiconducting thin films using long-chain aliphatic molecules on a SiO<sub>2</sub> gate insulator. In this paper, we demonstrate a stark contrast for a 2,5-bis(4-biphenyl)bithiophene (BP2T) active semiconducting layer grown on a modified SiO<sub>2</sub> dielectric gate insulator between two different modifications of tetratetracontane and poly(methyl methacrylate) thin films. Important evidence that the field effect transistor (FET) characteristics are independent of electrode metals with different work functions is given by the observation of a conversion of the metal-semiconductor contact from the Schottky limit to the Bardeen limit. An air-stable light emitting FET with an Au electrode is demonstrated.  
 © 2015 AIP Publishing LLC. [<http://dx.doi.org/10.1063/1.4927651>]

Carrier injection from metal electrodes to organic semiconductors is a process of a central importance in organic electronics and has been intensively studied from the point-of-view of device optimization by selecting electrodes with suitable work functions. Two limits are generally known in the metal-semiconductor (MS) contact, namely, the Schottky<sup>1</sup> and the Bardeen limits<sup>2,3</sup> [Fig. 1(a)]. The Schottky limit is most frequently observed for organic semiconductors with  $\pi$ -bond conjugated surfaces, while the Bardeen limit is typical for inorganic semiconductors with a covalent character such as silicon and germanium. In the former limit, the Schottky barrier height ( $\phi_b$ ) is very sensitive to the work function of the metal electrodes ( $\phi_m$ ), while this is not the case for the latter limit.<sup>2-5</sup> Both limits are considered to stem from different surface conditions. Inorganic semiconductors have dangling bonds on their surfaces and atomic-level reconstruction occurs, while almost no dangling bonds exist on organic semiconductor surfaces because the bulk consists of closed-shell molecules with van der Waals interactions. In many organic semiconductors, the injection and conduction of electrons are rarely observed. Instead, the transport of holes is more frequently observed for the following two reasons. One is that the Fermi level of Au, the most frequently used electrode, is generally close to the highest occupied molecular orbital (HOMO) of organic semiconductors, which allows easy access to hole carriers. The other is the fact that electrons are frequently trapped on the SiO<sub>2</sub> surface to prevent electric conduction even if they are injected from the electrodes.<sup>6</sup> Ambipolar carrier injection and transport in organic semiconductors were first reported for pentacene by Yasuda *et al.*<sup>7</sup> using Ca electrodes with a low work function and a parylene modifying layer on a SiO<sub>2</sub> substrate surface.

According to these conditions, ambipolar carrier injection and transport are presently considered to be a universal phenomenon in organic semiconductors,<sup>8-23</sup> and this efficient ambipolar action has opened an intriguing research area in organic light-emitting FETs (OLEFETs).

OLETs showing good performance have recently been reported in organic semiconductors using Ca-Au hetero-electrodes on a SiO<sub>2</sub> substrate with self-assembled monolayer or organic polymer surface modification, in which both hole and electron injection (so-called ambipolar characteristics) were achieved.<sup>10,16,18-23</sup> Metals with low  $\phi_m$ , however, are sensitive to oxygen and moisture, and therefore, devices containing Ca-Au hetero-electrodes cannot operate under ambient air conditions. Therefore, several attempts have been carried out in order to realize efficient ambipolar injection with Au electrodes. Some groups have reported efficient ambipolar injection with Au electrodes by employing a polymer semiconductor with a small band gap (1.25–1.43 eV) as an active layer.<sup>24-26</sup> However, this does not occur in typical molecular semiconductor materials with a larger band gap (generally ca. 2 eV), and their FET action is generally limited to only p-type characteristics in the case of Au electrodes.<sup>7</sup> This can be explained by the large energy difference between the HOMO-derived band of semiconductors and the Fermi level of the Au electrode.

Here, we show that another crucial control is possible for carrier injection by gate insulator surface control followed by thin film growth of an organic semiconductor. We present strong evidence that the Schottky limit most frequently found in organic semiconductors can be converted to the Bardeen limit by such surface modifications. A good example is given for 2,5-bis(4-biphenyl)bithiophene<sup>27</sup> (BP2T, see Fig. 1) organic semiconducting active layer grown on an aliphatic tetratetracontane (TTC)-modified SiO<sub>2</sub> dielectric gate insulator (TTC-SiO<sub>2</sub>). Although effective

<sup>a)</sup>Authors to whom correspondence should be addressed. Electronic addresses: kanagasekaran@gmail.com; Shimotani@m.tohoku.ac.jp; and tanigaki@m.tohoku.ac.jp.

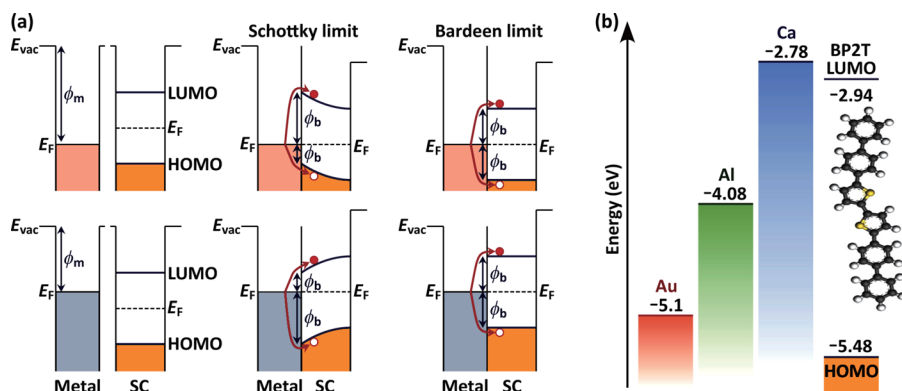


FIG. 1. (a) Schematic band diagrams of the metal semiconductor (MS) interface in the Schottky and the Bardeen limits. The top and the bottom objects represent metal electrodes with high and low work functions, respectively. The MS interface varies from the Schottky to the Bardeen limit depending on the semiconductor surface. (b) The work functions of Au, Al, Ca, and the energetic levels of LUMO- and HOMO-derived bands of the BP2T solid.

TTC modification on a substrate was tentatively suggested earlier without any clear reasoning,<sup>28</sup> in the present study we will give strong evidence that the Bardeen limit can be realized from two key experiments, namely, changing metal electrodes with different  $\phi_m$  and determining the band diagram by photoelectron yield spectroscopy (PYS). Well-balanced ambipolar carrier injection is clearly shown and air-stable light emission from FETs is demonstrated.

BP2T purchased from Sigma-Aldrich Co. LLC was purified by five times using a physical vapour transport method under a pure argon gas flow. BP2T transistors were fabricated on an n-type highly doped silicon ( $n^{++}$ -Si) substrate with a 200 nm-thick  $\text{SiO}_2$  layer as a gate electrode and a dielectric layer. The substrates were cleaned by ultrasonication in acetone, ethanol, and 2-propanol followed by  $\text{O}_2$ -plasma treatment. The substrate was subsequently modified by spin-coating poly(methyl methacrylate) (PMMA) with 60 nm or by thermally deposited TTC<sup>28</sup> with 9 nm in thickness. The PMMA and TTC layers were taken into account in calculating the capacitance of the gate insulators. The BP2T thin film (30 nm) was deposited by a vacuum vapor deposition method.<sup>27</sup> Thin film transistors were made by evaporating highly purified molecules under high vacuum ( $10^{-6}$  Torr), and the thickness was measured *in situ* by a quartz crystal microbalance. The thin film deposition rate was maintained at  $0.1 \text{ \AA/s}$ , and the substrate was kept at room temperature. Interdigitated electrodes of Au, Al, or Ca were deposited onto the thin films by vacuum vapor deposition with a shadow mask. The channel length and the width were  $100 \mu\text{m}$  and  $12000 \mu\text{m}$ , respectively. Source and drain electrodes of Au-Au, Ca-Ca, Al-Al, and Au-Ca with different  $\phi_m$ 's were used. In four terminal configuration, the distance between the source and the drain electrodes and that of the two voltage probes were  $300 \mu\text{m}$  and  $80 \mu\text{m}$ , respectively. Device performances were measured with an Agilent B1500A semiconductor parameter analyzer. Light emission images were recorded using a CCD camera as reported elsewhere.<sup>27</sup>

The drain current ( $I_d$ )-drain voltage ( $V_d$ ) output characteristics of an FET of BP2T polycrystalline thin films grown on TTC- $\text{SiO}_2$  with Au-Au homo-electrodes are shown in Fig. 2(a). Surprisingly, good symmetric characteristics between holes and electrons were observed. In the hole conduction measurements under relatively large negative gate voltages ( $V_g$ 's), a pure unipolar action (the left-side of Fig. 2(a)) was observed. It is noted that  $I_d$  suddenly increased at around  $V_d = -80 \text{ V}$  as  $V_d$  increased further in the negative

direction when a small negative  $V_g$  was applied. This is a typical signature of ambipolar action when electrons begin to be simultaneously injected into the channel. On the other hand, under positive  $V_g$  (the right-side of Fig. 2(a)), the transistor operates in an electron transport mode with an equivalent field-effect electron mobility  $\mu_e$ . As in the case of the hole region, unipolar electron transport became predominant at large positive  $V_g$ 's, while additional hole injection became also apparent as  $V_d$  increased further in the positive direction under small  $V_g$ 's.

The equivalent evolution of the  $I_d$ 's as a function of  $V_d$  between p- and n-type characteristics with the same Au electrodes indicates that the injection barriers against holes and electrons are comparable. Taking into account the fact that the Fermi level of Au is close to the HOMO of BP2T [Fig. 1(b)], electron injection should be greatly suppressed compared to hole injection in the Schottky limit [Fig. 1(a)]. The highly symmetric injection of both electrons and holes observed in the present research indicates that the MS contact is now far from the Schottky limit but close to the Bardeen limit. This surprisingly equivalent carrier injection

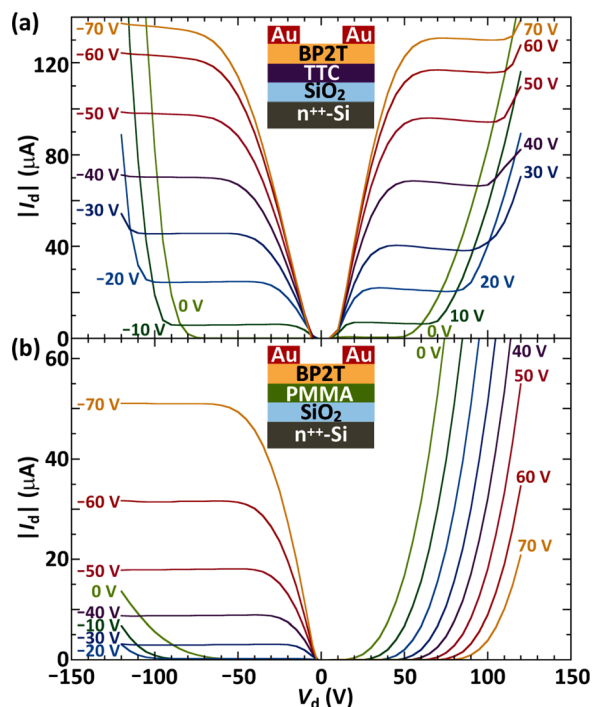


FIG. 2. The output characteristics of a BP2T FET with Au-Au homo-electrodes (a) on TTC- $\text{SiO}_2$  and (b) on PMMA- $\text{SiO}_2$ .

and conduction of holes and electrons is in sharp contrast to those of BP2T thin-film FETs on a SiO<sub>2</sub> dielectric layer coated with PMMA, as shown in Fig. 2(b). The p-type characteristics on the left-side of Fig. 2(b) show a behavior almost similar to that of the FET on TTC-SiO<sub>2</sub>. On the other hand, the n-type characteristics on the right-side of Fig. 2(b) are very different, in which electron conduction is too small to be seen on the scale of this plot, and therefore, one can see only hole injection in the region of large  $V_d$ . This extremely asymmetric carrier injection from the Au electrode to BP2T on a PMMA-SiO<sub>2</sub> substrate is striking evidence of the fact that the MS contact of BP2T-FETs falls within the Schottky limit.

It needs to be unambiguously confirmed whether the injection limit is indeed changed from the Schottky to the Bardeen limit, or whether this effect is merely caused by other factors such as carrier trapping at the interface between the semiconductor and the modification layer. First, we give clear phenomenological experimental evidence that work function ( $\phi_m$ ) of the electrodes does not give any significant influence on the carrier injection in BP2T FETs on TTC-SiO<sub>2</sub>. In order to clarify this issue, we compared the  $I_d$ - $V_g$  curves (transfer characteristics) of BP2T-FETs fabricated on TTC-SiO<sub>2</sub> [Fig. 3(a)] and on PMMA-SiO<sub>2</sub> [Fig. 3(b)] by employing Au-Au, Al-Al, and Ca-Ca homo-electrodes with different  $\phi_m$ 's in addition to the Au-Ca hetero-electrode under a constant  $V_d$  of 120 V. It is important to note that for making correct interpretations of the present experiments, carrier transport in the channel should ideally be the same in the vicinity of the interface between the semiconductor and the modification layers regardless of electrodes, because the metal electrodes were deposited after the deposition of BP2T on TTC-SiO<sub>2</sub> or PMMA-SiO<sub>2</sub> with the same substrate modifications. Therefore, differences observed in the transfer ( $I_d$ - $V_d$ ) characteristics can be solely attributed to the MS contact but not to the channel conduction around the interface between the semiconductor and the modification layer.

Typical ( $I_d$ )<sup>1/2</sup>- $V_g$  curves are plotted in Figs. 3(a) and 3(b), where one can see a strong contrast between the BP2T/TTC-SiO<sub>2</sub> and the BP2T/PMMA-SiO<sub>2</sub> characteristic curves. The p-type threshold voltage of the BP2T/PMMA-SiO<sub>2</sub> FETs showed a significant negative shift on decreasing  $\phi_m$  from Au to Ca, whereas the n-type threshold voltage showed a significant positive shift in the case of Au-Au electrodes,

indicating a significant change in the carrier injection barrier heights.<sup>29-32</sup> As a result, the minima of the  $I_d$ - $V_g$  transfer characteristics are widely distributed from  $V_g = 1.5$  V to 112 V with a strong dependence on the  $\phi_m$  of the electrodes. On the other hand, the threshold voltages of the BP2T/PMMA-SiO<sub>2</sub> FETs showed shifts in the same direction with a much weaker dependence on  $\phi_m$ . That leads to a narrow distribution of the  $I_d$  minima around  $V_G = 60$  V, which is the value expected for FETs with balanced p-type and n-type characteristics. The behavior is indicative of the fact that the carrier injection barriers are affected less by  $\phi_m$ . It is noted that Al is a very sensitive metal, and the first surface layer is affected by the contamination of oxygen on the surface. The off-trend behavior observed in the case of Al may arise from this reason.

For further convincing evidence, the  $\mu_e$  and  $\mu_h$  estimated from the saturation regions of the FET characteristics are shown in Fig. 3(c). The plot shows a clear difference between TTC-SiO<sub>2</sub> and PMMA-SiO<sub>2</sub> FETs. The FETs of BP2T on TTC-SiO<sub>2</sub> showed high field-effect mobilities for both holes and electrons, being nearly independent of the  $\phi_m$ 's of the electrodes. On the other hand, the mobilities of BP2T fabricated on PMMA-SiO<sub>2</sub> showed a large dependence upon the  $\phi_m$ , and consequently, the data are located in a wide area of the plot. This should be compared to the experimental results for FETs on PMMA-SiO<sub>2</sub>, where holes are predominantly injected from the Au electrode because of its  $\phi_m$  is close to the HOMO of BP2T (-5.48 eV, Fig. 1(b)), and similarly electrons are preferentially injected from the Ca electrode because of its  $\phi_m$  close to the lowest unoccupied molecular orbital (LUMO) (-2.94 eV, Fig. 1(b)). The mobilities experimentally observed for BP2T FETs in Fig. 3(c) are fairly consistent with the expected results from both limits.

We measured the contact resistance of the Au-Au homo electrode devices for both BP2T/TTC-SiO<sub>2</sub> and BP2T/PMMA-SiO<sub>2</sub> with a four-probe method, as shown in Fig. 4. The source contact resistance for hole injection is similar for both BP2T/TTC-SiO<sub>2</sub> and BP2T/PMMA-SiO<sub>2</sub>. Importantly, for electron injection, much smaller source resistance was observed for BP2T/TTC-SiO<sub>2</sub> than that for BP2T/PMMA-SiO<sub>2</sub>, which is consistent with the tendency of a change in MS contact limit.

In order to acquire unambiguous spectroscopic insights into the MS contact in addition to the phenomenological

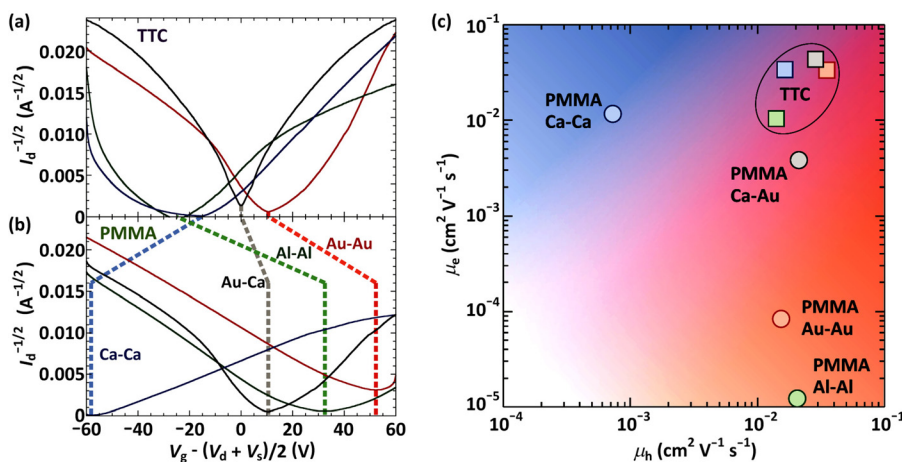


FIG. 3. (a) Transfer characteristics of BP2T FETs with various electrodes on TTC-SiO<sub>2</sub> and (b) on PMMA-SiO<sub>2</sub>. Operations of p- and n-modes measured in the range of  $V_d \leq 0$  V and  $V_d \geq 0$  V are shown in the same panel, which are controlled by various  $V_g$ 's under constant  $V_d$  of 120 V. The  $V_g$  is expressed by using an off-set value of  $(V_d + V_s)/2$ . (c) Field-effect mobilities of BP2T FETs. Electron ( $\mu_e$ ) and hole ( $\mu_h$ ) mobilities of BP2T FETs made on a SiO<sub>2</sub> substrate modified with TTC (squares) and PMMA (circles) are plotted.



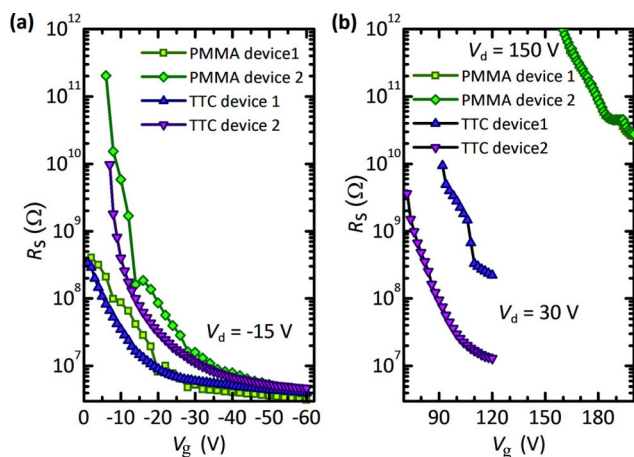


FIG. 4. (a) The source contact resistance for hole injection in BP2T/TTC/Au-Au and BP2T/PMMA/Au-Au. (b) The source contact resistance for electron injection in BP2T/TTC/Au-Au and in BP2T/PMMA/Au-Au.

understanding described earlier, we carried out PYS of Au/BP2T interface on both PMMA-SiO<sub>2</sub> and TTC-SiO<sub>2</sub>. The change in the surface modification layer is reflected in a change in the barrier ( $\phi_b$ ) values of electron injection, which were evaluated to be 0.96 and 1.10 eV at the Au/BP2T interface on PMMA-SiO<sub>2</sub> and on TTC-SiO<sub>2</sub>, respectively, as displayed in Fig. 5(a). The value of  $\phi_b = 0.96$  eV of the Au/BP2T interface on PMMA-SiO<sub>2</sub> was nearly equal to the difference between the Fermi level of Au thin film and the energy level of the BP2T HOMO-derived band (0.97 eV). This indicates that the interface is very close to the Schottky limit. On the other hand,  $\phi_b$  for the Au/BP2T interface on TTC-SiO<sub>2</sub> significantly shifted from 0.97 eV, indicating deviation from the Schottky limit. Detailed discussion about the PYS analyses is given in the supplementary material (see S1, Ref. 33).

Two different injection limits can be caused by the surface morphology of the thin films near the electrodes, as supported by X-ray diffraction (see S2, Ref. 33) and SEM measurements (see S3, Ref. 33) of BP2T thin films on TTC-SiO<sub>2</sub> and on PMMA-SiO<sub>2</sub>. The linewidth of their diffraction

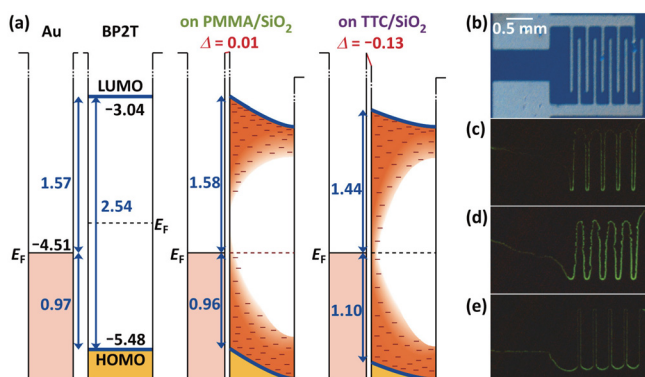


FIG. 5. (a) Band diagram of Au and BP2T in eV without contact (left), and a Au-BP2T interface on PMMA-SiO<sub>2</sub> (center) and TTC-SiO<sub>2</sub> (right).  $E_F$  and  $\Delta$  denote the Fermi level and the potential drop at the interface, respectively. The lines inside the red zone in color indicate the gap states. (b-e) Light emission images of a BP2T FET with Au-Au electrodes on TTC-SiO<sub>2</sub> with different gate voltages. (b) A top view of the FET with interdigitated electrodes. (c) Electroluminescence near the left electrode. (d) Electroluminescence from middle of the channel. (e) Electroluminescence near the right electrode.

peaks at  $2\theta = 13.46^\circ$  was  $0.230^\circ$  and  $0.201^\circ$  (see, Fig. S2), and their volume-weighted average crystallite sizes calculated with the Scherrer equation were 51.5 nm and 59.0 nm, respectively. The experimental fact that the BP2T thin film on PMMA-SiO<sub>2</sub> has higher crystallinity than that on TTC-SiO<sub>2</sub> is consistent with a smaller number of gap states in PMMA-SiO<sub>2</sub>.

By employing the Bardeen limit of the MS contact realized on TTC-SiO<sub>2</sub>, we demonstrated bright light emission in an organic FET with Au-Au homo-electrodes, as shown in Fig. 5(b). The light emission zone moved between the source and drain electrodes depending on  $V_g$  at constant  $V_d$ . This clearly shows that both electrons and holes are simultaneously injected and that the carrier recombination zone, which corresponds to the p-n junction to be structurally constructed in the case of conventional inorganic light-emitting diodes, can be automatically created without fabricating any artificial p-n junctions. The critical phenomenological evidence for the conversion from the Schottky to the Bardeen limits in the MS contact of organic semiconductors was experimentally shown from metal electrodes with various  $\phi_m$ 's. A band diagram was described in connection to the Bardeen and the Schottky limits of carrier injection. Both electrons and holes were simultaneously injected into BP2T-FETs fabricated on TTC-SiO<sub>2</sub> with Au electrodes, almost independently of the  $\phi_m$ 's of the electrodes. The present studies provided a deep scientific insight into the MS-contact limits and will open a way to achieve high performance OLETs operating in air.

T.K. would like to thank JSPS research fellow scholarship during the present studies. H.S. is grateful to CSC scholarship from Chinese government as well as a scholarship from Tohoku University for research and education. This work was supported by JSPS KAKENHI Grant Nos. 24684023 and 25610084.

<sup>1</sup>W. Schottky, *Z. Phys.* **118**, 539 (1942).

<sup>2</sup>J. Bardeen, *Phys. Rev.* **71**, 717 (1947).

<sup>3</sup>J. Bardeen and W. H. Brattain, *Phys. Rev.* **75**, 1208 (1949).

<sup>4</sup>S. Kurtin, T. C. McGill, and C. A. Mead, *Phys. Rev. Lett.* **22**, 1433 (1969).

<sup>5</sup>B. Jaeckel, J. B. Sambur, and B. A. Parkinson, *J. Appl. Phys.* **103**, 063719 (2008).

<sup>6</sup>L.-L. Chua, J. Zaumseil, J.-F. Chang, E. C.-W. Ou, P. K.-H. Ho, H. Sirringhaus, and R. H. Friend, *Nature* **434**, 194 (2005).

<sup>7</sup>T. Yasuda, T. Goto, K. Fujita, and T. Tsutsui, *Appl. Phys. Lett.* **85**, 2098 (2004).

<sup>8</sup>J. S. Swensen, C. Soci, and A. J. Heeger, *Appl. Phys. Lett.* **87**, 253511 (2005).

<sup>9</sup>Th. B. Singh, F. Meghdadi, S. Günes, N. Marjanovic, G. Horowitz, P. Lang, S. Bauer, and N. S. Sariciftci, *Adv. Mater.* **17**, 2315 (2005).

<sup>10</sup>J. Zaumseil, R. H. Friend, and H. Sirringhaus, *Nat. Mater.* **5**, 69 (2006).

<sup>11</sup>J. Zaumseil, C. L. Donley, J.-S. Kim, R. H. Friend, and H. Sirringhaus, *Adv. Mater.* **18**, 2708 (2006).

<sup>12</sup>T. Takahashi, T. Takenobu, J. Takeya, and Y. Iwasa, *Appl. Phys. Lett.* **88**, 033505 (2006).

<sup>13</sup>M. H. Yoon, C. Kim, A. Facchetti, and T. J. Marks, *J. Am. Chem. Soc.* **128**, 12851 (2006).

<sup>14</sup>S. Seo, B. M. Park, and P. G. Evans, *Appl. Phys. Lett.* **88**, 232114 (2006).

<sup>15</sup>T. Sakanoue, M. Yahiro, C. Adachi, H. Uchiuzou, T. Takahashi, and A. Toshimitsu, *Appl. Phys. Lett.* **90**, 171118 (2007).

<sup>16</sup>T. Takenobu, S. Z. Bisri, T. Takahashi, M. Yahiro, C. Adachi, and Y. Iwasa, *Phys. Rev. Lett.* **100**, 066601 (2008).

<sup>17</sup>T. Takenobu, K. Watanabe, Y. Yomogida, H. Shimotani, and Y. Iwasa, *Appl. Phys. Lett.* **93**, 073301 (2008).

<sup>18</sup>S. Z. Bisri, T. Takenobu, Y. Yomogida, H. Shimotani, T. Yamao, S. Hotta, and Y. Iwasa, *Adv. Funct. Mater.* **19**, 1728 (2009).

- <sup>19</sup>Y. Wang, R. Kumashiro, Z. R. Li, R. Nouchi, and K. Tanigaki, *Appl. Phys. Lett.* **95**, 103306 (2009).
- <sup>20</sup>Y. Wang, R. Kumashiro, R. Nouchi, N. Komatsu, and K. Tanigaki, *J. Appl. Phys.* **105**, 124912 (2009).
- <sup>21</sup>Y. Yomogida, T. Takenobu, H. Shimotani, K. Sawabe, S. Z. Bisri, T. Yamao, S. Hotta, and Y. Iwasa, *Appl. Phys. Lett.* **97**, 173301 (2010).
- <sup>22</sup>S. Hotta, T. Yamao, S. Z. Bisri, T. Takenobu, and Y. Iwasa, *J. Mater. Chem. C* **2**, 965 (2014).
- <sup>23</sup>S. Z. Bisri, C. Piliago, J. Gao, and M. A. Loi, *Adv. Mater.* **26**, 1176 (2014).
- <sup>24</sup>W. Hong, B. Sun, H. Aziz, W.-T. Park, Y.-Y. Nohd, and Y. Li, *Chem. Commun.* **48**, 8413 (2012).
- <sup>25</sup>J. Lee, A.-R. Han, J. Kim, Y. Kim, J. H. Oh, and C. Yang, *J. Am. Chem. Soc.* **134**, 20713 (2012).
- <sup>26</sup>H.-W. Lin, W.-Y. Lee, and W.-C. Chen, *J. Mater. Chem.* **22**, 2120 (2012).
- <sup>27</sup>K. Oniwa, T. Kanagasekaran, T. Jin, Md. Akhtaruzzaman, Y. Yamamoto, H. Tamura, I. Hamada, H. Shimotani, N. Asao, S. Ikeda, and K. Tanigaki, *J. Mater. Chem. C* **1**, 4163 (2013).
- <sup>28</sup>M. Kraus, S. Haug, W. Brütting, and O. Andreas, *Org. Electron.* **12**, 731 (2011).
- <sup>29</sup>R. Schroeder, L. A. Majewski, and M. Grell, *Appl. Phys. Lett.* **83**, 3201 (2003).
- <sup>30</sup>K. Kanai, M. Honda, H. Ishii, Y. Ouchi, and K. Seki, *Org. Electron.* **13**, 309 (2012).
- <sup>31</sup>R. T. Tung, *Mater. Sci. Eng., R* **35**, 1 (2001).
- <sup>32</sup>M. G. Helander, Z. B. Wang, J. Qiu, and Z. H. Lu, *Appl. Phys. Lett.* **93**, 193310 (2008).
- <sup>33</sup>See supplementary material at <http://dx.doi.org/10.1063/1.4927651> for S1: Band Diagrams determined by Photoelectron Yield Spectra, S2: X-ray diffraction measurements of BP2T thin films on PMMA-SiO<sub>2</sub> and on TTC-SiO<sub>2</sub>, and S3: SEM analysis.